OPEN ACCESS Freely available online

PLoS GENETICS

Zebrafish *usp39* Mutation Leads to *rb1* mRNA Splicing Defect and Pituitary Lineage Expansion

Yesenia Ríos[1], Shlomo Melmed[2], Shuo Lin[1]*, Ning-Ai Liu[2]*

1 Department of Molecular, Cell, and Developmental Biology, University of California Los Angeles, Los Angeles, California, United States of America, **2** Department of Medicine, Cedars-Sinai Medical Center, University of California Los Angeles, Los Angeles, California, United States of America

Abstract

Loss of retinoblastoma (Rb) tumor suppressor function is associated with human malignancies. Molecular and genetic mechanisms responsible for tumorigenic Rb downregulation are not fully defined. Through a forward genetic screen and positional cloning, we identified and characterized a zebrafish *ubiquitin specific peptidase 39 (usp39)* mutation, the yeast and human homolog of which encodes a component of RNA splicing machinery. Zebrafish *usp39* mutants exhibit microcephaly and adenohypophyseal cell lineage expansion without apparent changes in major hypothalamic hormonal and regulatory signals. Gene expression profiling of *usp39* mutants revealed decreased *rb1* and increased *e2f4*, *rbl2 (p130)*, and *cdkn1a (p21)* expression. Rb1 mRNA overexpression, or antisense morpholino knockdown of *e2f4*, partially reversed embryonic pituitary expansion in *usp39* mutants. Analysis of pre-mRNA splicing status of critical cell cycle regulators showed misspliced Rb1 pre-mRNA resulting in a premature stop codon. These studies unravel a novel mechanism for *rb1* regulation by a neuronal mRNA splicing factor, *usp39*. Zebrafish *usp39* regulates embryonic pituitary homeostasis by targeting *rb1* and *e2f4* expression, respectively, contributing to increased adenohypophyseal sensitivity to these altered cell cycle regulators. These results provide a mechanism for dysregulated *rb1* and *e2f4* pathways that may result in pituitary tumorigenesis.

Citation: Ríos Y, Melmed S, Lin S, Liu N-A (2011) Zebrafish *usp39* Mutation Leads to *rb1* mRNA Splicing Defect and Pituitary Lineage Expansion. PLoS Genet 7(1): e1001271. doi:10.1371/journal.pgen.1001271

Editor: James Amatruda, University of Texas Southwestern, United States of America

Received March 24, 2010; **Accepted** December 8, 2010; **Published** January 13, 2011

Funding: This research was supported by grants from the National Institutes of Health 1F31DK0653620 (YR), RR13227 (SL), and KO8 DK064806 (NAL). The funders had no role in study design, data collection and analysis, decision to publish, or preparation of the manuscript.

Competing Interests: The authors have declared that no competing interests exist.

* E-mail: shuolin@ucla.edu (SL); liuna@cshs.org (NAL)

Introduction

The hypothalamic-pituitary axis regulates stress responses, growth, reproduction and energy homeostasis. Neuropeptides released from the hypothalamus via the hypophyseal portal plexus control synthesis and secretion of anterior pituitary hormones [1]. Different pituitary cell types secrete hormones that regulate postnatal growth (growth hormone, GH), lactation (prolactin, PRL), metabolism (thyroid stimulating hormone, TSH), stress (adrenocorticotrophic hormone, ACTH), pigmentation (melanocyte-stimulating hormone, αMSH), sexual development and reproduction (luteinizing hormone, LHβ, and follicle stimulating hormone, FSHβ) [2]. Corticotropes and melanotropes produce proopiomelanocortin (POMC), which is proteolytically cleaved to give rise to ACTH in corticotropes and αMSH in melanotropes.

Central and peripheral signals including hypothalamic stimulatory hormones, growth factors and estrogen cause pituitary hyperplasia, genetic instability, subsequent monoclonal growth expansion and tumor formation [3]. Pituitary tumors are almost invariably benign, however if untreated, they are associated with increased morbidity and mortality due to tumor mass effect and/or hormonal disruptions leading to serious complications such as acromegaly and Cushing's disease [4,5]. How developmental or acquired signals elicit plastic change in pituitary cell growth resulting in hyperplasia or benign adenomas is not fully understood [6].

The pituitary gland is highly sensitive to cell cycle regulators including cyclins, cyclin dependent kinases (CDKs), CDK inhibitors (CKIs) and retinoblastoma protein (pRB), all of which are frequently dysregulated in pituitary tumors. pRB, a nuclear pocket protein, binds the E2F transcription factors and regulates the balance between cell quiescence and proliferation [7]. E2Fs control expression of genes crucial for cell cycle re-entry, DNA replication and mitosis. Dephosphorylated pRB binds to E2Fs and inhibits transcription of E2F target genes either by sequestration and inhibition of E2F cell cycle "activators" (E2F1–E2F3), or by formation of pocket protein complexes with "inhibitors" (E2F4–E2F8), which bind to E2F-responsive promoters and repress their transcription [7]. Accordingly, transcriptional repression of pRB activity prevents G1/S progression and promotes cell quiescence.

In mice, *Rb* heterozygous mutations lead to early onset and increased incidence of endocrine neoplasma including pituitary, thyroid and adrenal tumors [8,9]. The 100% penetrance of pituitary tumors in $Rb^{+/-}$ mice [8] is partially reversed in $Rb^{+/-}$; $E2f4^{-/-}$ double mutants, implicating the *Rb/E2f4* pathway in pituitary tumorigenesis and also suggesting an E2F4 oncogenic activity [9]. E2F4 is also known as a key regulator associated with p130 in G0/G1 to promote quiescent G0 and terminal differentiation [10,11]. *E2f4* null mice often die shortly after birth with defects of terminal differentiation resulting from an inability to establish cell cycle quiescence [12]. In response to cell cycle re-entry, E2F4 switches from p130 [10,13] to pRB [10,14] and p107 [10,14,15], which inhibit E2F4 transactivation. Additionally, E2F4 overexpression has been shown to promotes cell proliferation and transformation [14,15], which prevents growth arrest mediated by p130 [13].

Author Summary

Previous studies have shown that $Rb^{+/-}$ mice develop pituitary adenomas; however, *RB1* mutations have not been found in human pituitary tumors. In the present study, we uncovered a novel genetic pathway that may lead to Rb downregulation through RNA splicing mediated by *usp39*, a gene involved in assembly of the spliceosome. Our forward genetic study in zebrafish suggests that loss of *usp39* results in aberrant *rb1* mRNA splicing, which likely causes elevated expression of its target *e2f4*, a key regulator known to have oncogenic activity when overexpressed. We established that *e2f4* upregulation is a main factor responsible for the adenohypophyseal cell lineage hyperplasia observed in the zebrafish *usp39* mutant. It should be of interest to investigate if mutations or downregulation of *USP39* would contribute to pituitary tumorigenesis in humans.

Pituitary development and physiology are conserved in zebrafish [2]. Novel insights into developmental mechanisms have been obtained by *in vivo* analysis of transgenic zebrafish expressing GFP and RFP driven by regulatory elements of zebrafish *pomc* [16] and *prl* [17], respectively. Through a forward genetic screen for novel zebrafish genes regulating adenohypophyseal *pomc* gene expression, we identified and characterized a mutant that harbors a nonsense mutation in *usp39*, leading to expansion of all adenohypophyseal cell lineages.

Usp39 encodes a conserved protein termed Sad1p in *Saccharomyces cerevisiae* and a 65 kDa (65K) SR-related protein in humans [18,19]. Both yeast Sad1p and the 65K SR-related protein in humans are involved in assembly of the spliceosome, the RNA splicing machinery [18,19]. RNA splicing is crucial for eukaryotic gene expression and defective splicing can be detrimental since it leads to an altered genetic message [20]. The spliceosome consists of five small nuclear ribonucleoproteins (snRNPs), U1, U2, U4, U5 and U6 as well as a large number of non-snRNP proteins [20]. The yeast Sad1p is involved in splicing *in vivo* and *in vitro* and in the assembly of U4 snRNP to U6 snRNP [18], while human 65K SR-related protein is essential for recruitment of the tri-snRNP to the pre-spliceosome and is known as a tri-snRNP-specific protein [19,21]. Additionally, Usp39 is also classified as a deubiquitinating enzyme but lacks protease activity due to absence of key active-site residues of cysteine and histidine [18,19,22].

In the present study, we aimed to define novel pathways regulating pituitary development through study of an *usp39* mutation. Using microarray gene expression profiling followed by quantitative real time-polymerase chain reaction (RT-PCR) validation we observed a significant reduction of *rb1* expression and increased *e2f4*, *rbl2 (p130)* and *cdkn1a (p21)* expression in mutants. Zebrafish *usp39* is predominantly expressed in the brain and represents a novel neuronal splicing factor. We show that zebrafish *usp39* mutation leads to an *rb1* splicing defect responsible for pituitary expansion. In addition, knockdown of *e2f4* partially rescued *pomc* lineage expansion in *usp39* mutants. Our finding that *usp39* regulates expansion of all embryonic pituitary cell lineages through the *rb1/e2f4* pathway may shed light on mechanisms underlying adult pituitary tumor formation.

Results

The *hp689* locus encodes *usp39*

To isolate genes required for adenohypophysis and hypothalamic development a standard forward genetics method was carried out using a three-generation (F3) screen after mutagenesis with ENU, which mostly induces single nucleotide exchanges at random positions of the genome [23–25]. The genetic screen was performed using *pomc* expression as a specific marker. *pomc is* expressed in subepithelial pituitary cells, dorsal to the oral ectoderm roof and ventral to the ventral diencephalon. A subset of *pomc*-expressing cells is also located outside the adenohypophysis, corresponding to β-endorphin-synthesizing cells of the hypothalamic arcuate nucleus [2]. In zebrafish, spatial distribution of the six different hormone secreting pituitary cell types is subdivided into three regions along the antero-posterior adenohypophyseal axis of the rostral pars distalis, proximal pars distalis and pars intermedia [2]. *pomc* is expressed in corticotropes of the rostral pars distalis, in melanotropes of the pars intermedia and in the hypothalamus (Figure 1A).

We isolated an ENU-induced mutant, *hp689*, which was characterized by reduced hypothalamic but increased pituitary *pomc* expression at 48-hours post fertilization (hpf) (Figure 1B). In addition, *hp689* mutants displayed microcephaly and smaller eyes starting at 33 hpf (data not shown). Using segregation linkage analysis, the *hp689* locus was mapped to zebrafish linkage group 5 with a critical interval of 0.03 centimorgan (cM) on marker ndrg3 (Figure 1C, see *Materials and Methods*). This region contained 7 annotated genes and sequencing of *usp39* from mutant embryos revealed a point mutation that converted a TAT codon into a TAA in exon 11, resulting in a premature termination codon rather than a tyrosine amino acid (Figure 1D). PROSITE database search of the Usp39 protein revealed two domains consisting of a zinc finger (ZF_UBP) and a Ubiquitin carboxyl-terminal hydrolases family 2 (UCH_2_3) region [26]. As a result of the UCH_2_3 domain, Usp39 is classified as a deubiquitinating enzyme. However, it lacks protease activity due to the absence of key active site cysteine and histidine residues [18,19,22]. The single allele of *hp689* carries a nonsense mutation within the UCH_2_3 region, resulting in a truncated Usp39 protein lacking amino acids after position 412 (Figure 1D).

To confirm that *hp689* represents the *usp39* mutation, a *usp39* antisense morpholino (MO) oligonucleotide targeting the *usp39* start codon and consequentially blocking translation was injected into wild-type (wt) embryos [27]. MO injected embryos showed increased *pomc* expression, similar to the *hp689* phenotype (Figure 1F compared to Figure 1B). Furthermore, injection of mRNA encoding wild-type *usp39* rescued the mutant phenotype (Table 1), indicating that pituitary *pomc* upregulation in *usp39* mutants results from the nonsense mutation in zebrafish *usp39*.

usp39 is predominantly expressed in the zebrafish embryonic brain

RNA whole-mount *in situ* hybridization was performed to determine the spatiotemporal expression pattern of *usp39* during zebrafish development. Generally weak *usp39* expression was detected in early cleavage embryos (data not shown) but tissue specific expression peaked by 36 hpf and decreased by 42 hpf (Figure 2A–2C). Expression was detected predominantly within the brain, including the pituitary region and eyes. At 21.5 hpf, there was also expression in the intermediate cell mass, the site of embryonic zebrafish hematopoiesis (Figure 2A, inset). However, mutants showed persistently lower *usp39* expression that was completely lost by 42 hpf (Figure 2D). In addition, loss of *usp39* expression by 42 hpf corresponds to the time at which the *usp39* mutant embryos fully develop a phenotype of microcephaly, smaller eyes and a pituitary abnormality, indicating the critical time point when *usp39* is required for normal development.

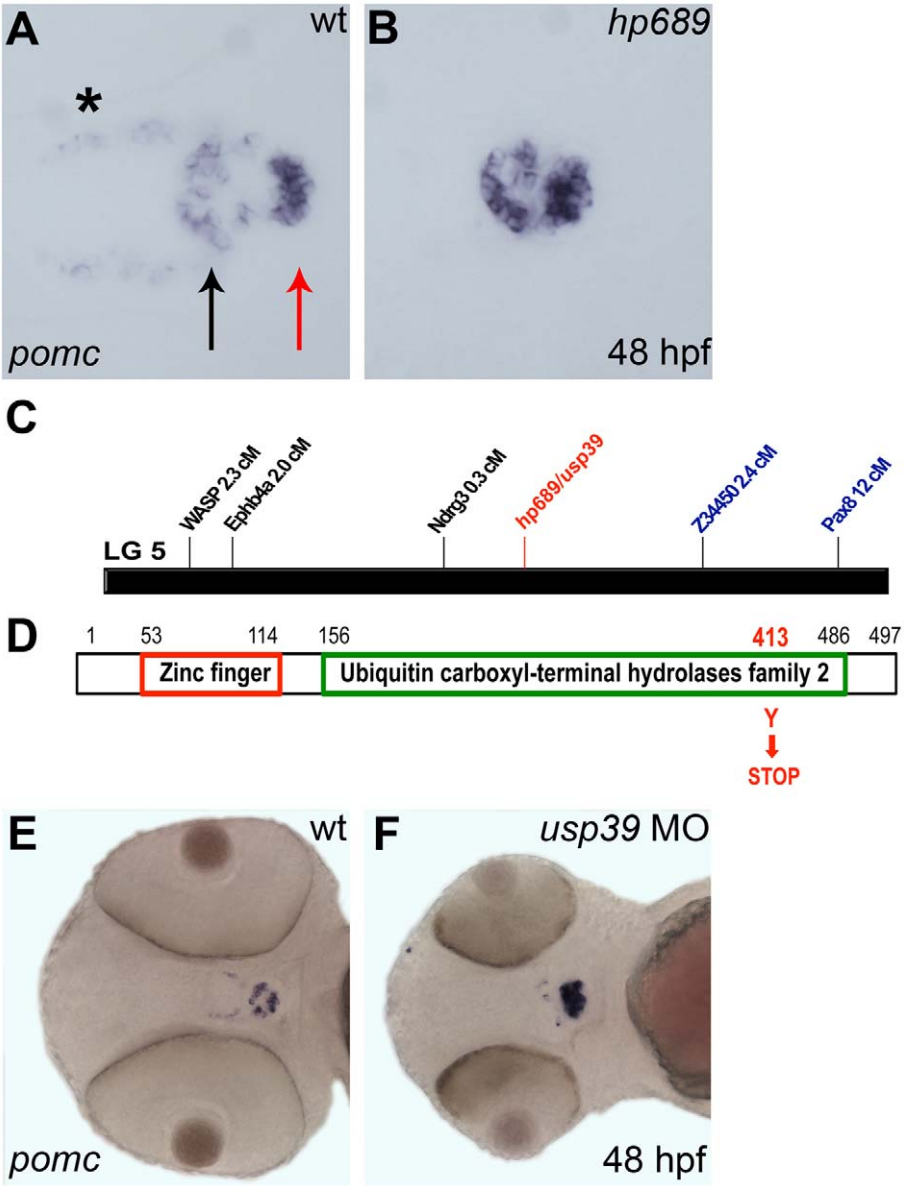

Figure 1. *hp689* is a novel zebrafish gene encoding *usp39*. A, B, E, F: Whole-mount *in situ* hybridization with *pomc* probe at 48 hpf, ventral view with anterior to left. (A) Wild-type (wt) embryo, *pomc* is expressed in the rostral pars distalis (black arrow), the pars intermedia (the red arrow), and in the β-endorphin-synthesizing neurons of the hypothalamus (asterisk). The medial domain which lacks *pomc* expression corresponds to the proximal pars distalis. (B) The *hp689* mutant exhibits increased *pomc* expression in the adenohypophysis, and lower expression in the hypothalamus compared to wt. (C) Genomic map of linkage group 5 (LG5) and position of the *hp689* mutation (in red) and mapping markers based on meiotic segregation linkage analysis. *hp689* mapped close to markers z34450 and ndrg3 that were located 2.4 cM and 0.3 cM, respectively (see *Materials and Methods*). (D) Schematic representation of the Usp39 protein, which include a zinc finger and ubiquitin carboxyl-terminal hydrolases family 2 domains with the *hp689* mutation from a tyrosine to a stop codon indicated in red. (E) Non-injected wt control embryos. (F) wt embryos injected with *usp39* MO. Note increased *pomc* expression and disorganization of the adenohypophysis similar to the increased expression of *pomc* in *usp39* mutant embryos in (B).
doi:10.1371/journal.pgen.1001271.g001

Table 1. *usp39* mRNA overexpression rescues the mutant *usp39* phenotype.

Injection	Total #	Mutant #	%
Control	161	38	24
usp39 mRNA	128	3	2

doi:10.1371/journal.pgen.1001271.t001

Pituitary cell lineage expansion in *usp39* mutants

The zebrafish adenohypophysis consists of six different hormone-secreting cell types distributed along the anterior-posterior axis: lactotropes and corticotropes are located anteriorly in the rostral pars distalis, thyrotropes, gonadotropes and somatotropes are found medially in the proximal pars distalis whereas melanotropes are situated posteriorly in the pars intermedia (Figure 3). To determine if additional pituitary lineages are affected by the *usp39* mutation, we performed double color RNA *in situ* hybridization analysis with combinatory pituitary

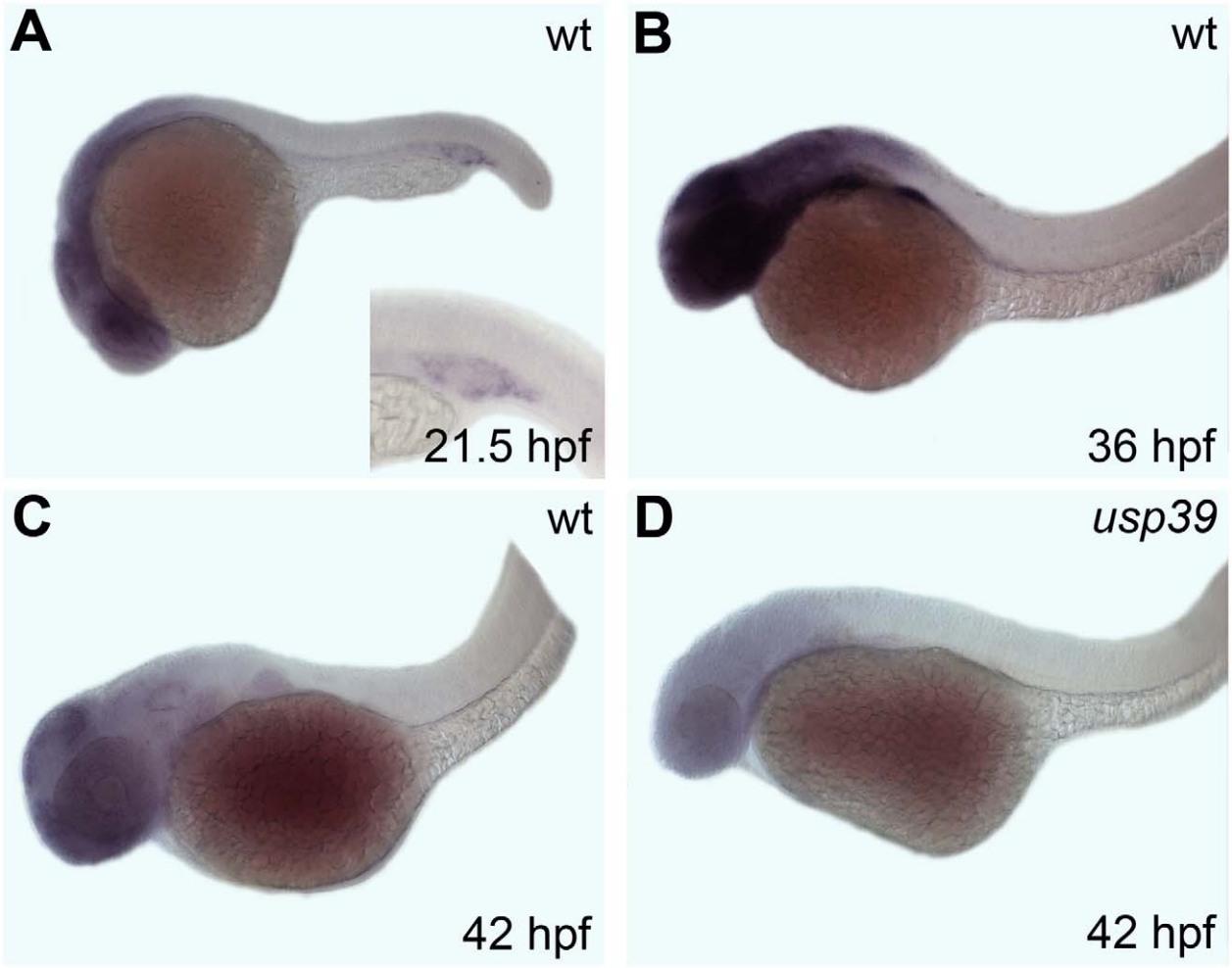

Figure 2. Whole-mount *in situ* hybridization analysis of the zebrafish *usp39* expression pattern. Embryonic ages are shown in the lower right corner, lateral view. A–C: Expression of *usp39* in wt is found in the brain and eye region. (A) Inset shows additional *usp39* expression in the intermediate cell mass, site of embryonic zebrafish hematopoiesis. (B) *usp39* expression is highest at 36 hpf. (C) *usp39* expression declines by 42 hpf. (D) The expression pattern of *usp39* in *usp39* mutants is lower in all stages; expression at 42 hpf is depicted.
doi:10.1371/journal.pgen.1001271.g002

lineage specific marker genes *pomc*, *gh*, *prl*, *tsh*, and with *cga* that encodes the glycoprotein α-subunit heterodimerizing with TSHβ, LHβ, or FSHβ subunit [2,16]. This analysis revealed expansion of all the analyzed cell lineages without apparent cell fate transformation in the *usp39* mutant pituitary at 48 hpf (Figure 3A–3P). Cell expansion was most marked in corticotropes and lactotropes, indicating that *usp39* is important for regulating embryonic pituitary cell populations (Figure 3B, 3D, 3F, 3H, 3J, and 3L).

Pituitary lineage expansion in *usp39* mutants is independent of hypothalamic releasing hormone and dopamine signals

We examined expression of hypothalamic regulators to investigate whether pituitary lineage expansion in *usp39* mutants is due to altered hypothalamic neuroendocrine input to the adenohypophysis. One of the primary hypothalamic inhibitory mechanisms controlling pituitary homeostasis is dopamine (DA) released from tuberoinfundibular neurons (TIDA). Pituitary lactotrophs are almost exclusively regulated by tonic inhibition of dopamine, which inhibits lactotroph proliferation, PRL gene expression and secretion by activating D2 dopamine receptor subtype (Drd2) [28]. We therefore processed 48 hpf whole-mount embryos for immunocytochemistry using an antibody against tyrosine-hydroxylase, the rate-limiting enzyme of dopamine synthesis in TIDA neurons, and detected no significant change of hypothalamic dopaminergic neurons in *usp39* mutants compared with wt siblings (Figure 4D and 4H). Corticotropin releasing hormone (CRH) as well as gonadotropin-releasing hormone (GnRH) stimulates cell growth, hormone synthesis and secretion of pituitary corticotropes and gonadotropes, respectively [29,30]. However, *usp39* mutants exhibit no altered *crh* or *gnrh* expression (Figure 4E–4G). Therefore, pituitary lineage expansion of *usp39* mutants occurs independently of major hypothalamic neuroendocrine signals.

Pituitary transcription factors are upregulated during late stage of development in *usp39* mutants

We next studied expression of transcription factors important for adenohypophyseal development. Lim3/Lhx3 is one of the earliest pituitary specifying transcription factors and is required for progenitor proliferation and survival [2]. Pitx3, a Pitx/Rieg

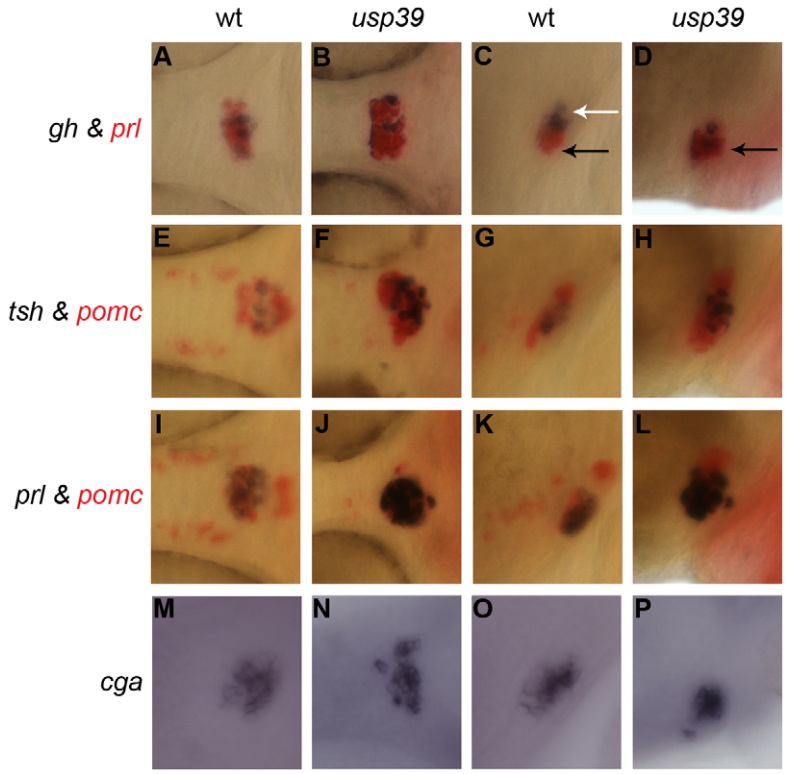

Figure 3. *usp39* mutation lead to expansion of all pituitary cell lineages at 48 hpf as indicated by pituitary hormone markers. A–L: Whole-mount double *in situ* hybridization with probes indicated on the side. *usp39* mutant embryos exhibit higher expression of all pituitary hormone markers compared to wild-type (wt) embryos. Spatial distribution of *prl*, *tsh*, *pomc* and *cga* are normal in the *usp39* mutant. (A, B, E, F, I, J, M, and N) ventral view and (C, D, G, H, K, L, O, and P) lateral view, with anterior to the left. Columns 1 (A, E, I, and M) and 3 (C, G, K and O) show wt siblings; columns 2 (B, F, J, and N) and 4 (D, H, L, and P) show *usp39* mutant embryos. A–D: *gh* (purple) and *prl* (red) transcripts. (C) The spatial distribution of *gh* is normally found in the proximal pars distalis (white arrow) and *prl* is found in the rostral pars distalis (black arrow). (D) Note the spatial distribution of *gh* in the *usp39* mutant; *gh* is abnormally expressed in the rostral pars distalis (black arrow). E–H: *tsh* (purple) and *pomc* (red) transcripts. I–L: *prl* (purple) and *pomc* (red) transcripts. M–P: Whole-mount *in situ* hybridization with *cga* transcript.
doi:10.1371/journal.pgen.1001271.g003

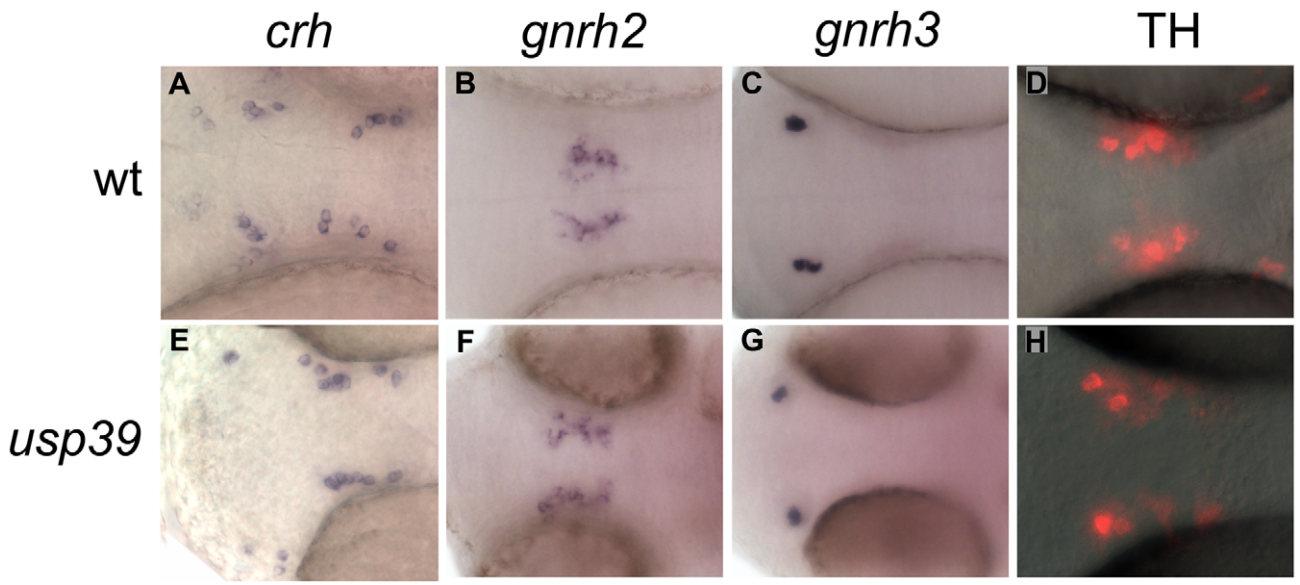

Figure 4. The hypothalamic releasing hormone and dopamine signals are unaffected in *usp39* mutants. A–C and E–G: Whole-mount *in situ* hybridization with hypothalamic probes at 48 hpf, ventral view. (A–C) wild-type (wt) embryos. (E–G) *usp39* mutant embryos. Expression of hypothalamic markers *crh*, *gnrh2*, and *gnrh3* did not change. D and H: Immunocytochemistry with tyrosine hydroxylase (TH) antibody at 48 hpf, ventral view. (H) Expression of TH in *usp39* mutant embryos did not change.
doi:10.1371/journal.pgen.1001271.g004

homeodomain protein, defines the pituitary placode and is required for Lim3 expression [2]. Pit1 is a Pou domain homeoprotein and a lineage-determining factor for somatotropes, lactotropes and thyrotropes [2]. The *Drosophila* eye absent homolog, *eya1*, is required for specification of gonadotropes, corticotropes, and melanotropes [2]. Zebrafish mutation of *ascl1a*, a homolog of the *Drosophila* MASH1 [31], resulted in failed endocrine differentiation of all adenohypohyseal cell types [2]. Expression of these zebrafish pituitary regulators coincides within the pituitary placode of the anterior neural ridge (ANR) at 20-somite stage (18 hpf) and persists in the adenohypophyseal anlage throughout 48 hpf (for *eya1*), or even later (for *pit1*, *lim3*, *pitx3*, and *ascl1a*). At 36 hpf, *usp39* mutants exhibited no increased expression of *lim3*, however *pit1*, *lim3*, *pitx3*, *eya1* and *ascl1a* showed a significant expression difference at a later state (48 hpf) compared with wt (Figure S1, Figure 5). These results suggest that the *usp39* mutation did not affect initial embryonic pituitary progenitor specification but induced their expansion after 36 hpf.

usp39 mutants exhibit altered expression of cell cycle regulators including *rb1* and *e2f4*

To distinguish whether the altered pituitary signals detected by whole-mount *in situ* hybridization is due to pituitary hyperplasia or higher expression of pituitary hormone levels we crossed *usp39* +/− fish to POMC-GFP transgenic fish [16]. After identifying mutant *usp39* in the POMC-GFP background, we sectioned *usp39* and wt whole embryos and performed immunocytochemistry with anti-GFP followed by cell number quantification. Our results demonstrated that there was an increase in the number of POMC-GFP-positive cells in *usp39* mutants compare to wt (Figure S2A–S2F). In addition, counting the nuclei stained with DAPI indicated an increase in the total number of pituitary cells in the *usp39* mutant compare to wt embryos (Figure S2G). We carried out a BrdU incorporation study and demonstrated that the increase in pituitary cell number seen in *usp39* mutants was due to an increase in proliferation (Figure S2H and S2I). It is well established that cell cycle dysregulation is associated with pituitary pathology in animal models and human disease [32]. However, little is known about mechanisms underlying the sensitivity of differentiated pituitary cell lineages to cell cycle regulators. We therefore performed a microarray analysis and focused on cell cycle regulators, 11 of which were confirmed for altered expression in *usp39* mutants by quantitative RT-PCR. In summary, expression levels of 3 genes were increased including *e2f4*, *rbl2 (p130)* and *cdkn1a (p21)* and expression of the other 8 cell cycle genes including *rb1* were downregulated (Table 2; Figure S3).

We further examined *e2f4* expression by RNA whole-mount *in situ* hybridization, which confirmed its upregulation in the adenohypophysis of *usp39* mutants compared to wt embryos (Figure 6A and 6B). To investigate whether *e2f4* upregulation is responsible for adenohypophysis lineage expansion, we injected embryos with antisense MO oligonucleotide to knockdown *e2f4* function. The overall *usp39* mutant phenotype maintained after *e2f4* MO injections, which resulted in partial reversal of *pomc* expansion in *e2f4*-MO-injected *usp39* embryos at 48 hpf compared to control embryos (Figure 6C–6E, mutant N = 20, ~60% showed rescue). The phenotypic rescue of *usp39* embryos by *e2f4*-MO is pituitary specific since *pomc* hypothalamic expression was not altered. In addition, we analyzed *prl* expression and a partial rescue was also observed in *e2f4*-MO-injected *usp39* embryos (Figure S4). These results indicate that loss of *usp39* results in increased *e2f4* expression, which at least partially contributes to the observed *pomc* lineage expansion in zebrafish adenohypophysis.

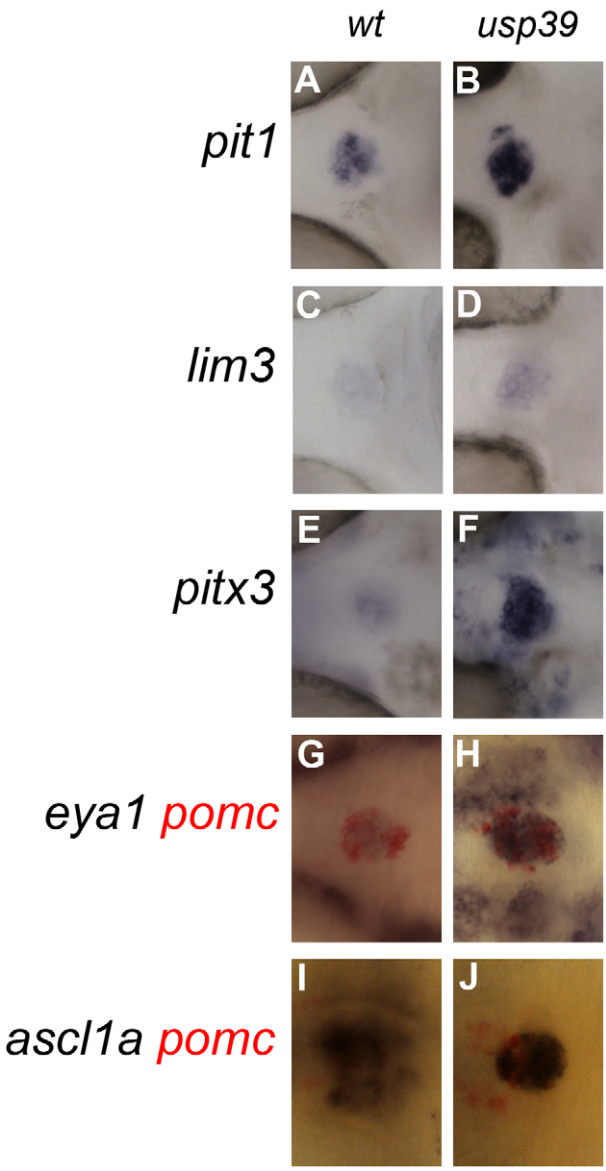

Figure 5. Loss of *usp39* leads to pituitary expansion as indicated by increased expression of pituitary transcription factors. A–F and G–J: Single and double *in situ* hybridization with probes indicated on the side, at 48 hpf, ventral view, anterior to the left. (A, C, E, G, and I) wild-type (wt) embryos. (B, D, F, H, and J) *usp39* mutant embryos have increased pituitary expression of *pit1*, *lim3*, *pitx3*, *eya1*, and *ascl1a*.
doi:10.1371/journal.pgen.1001271.g005

rb1 splicing defect contributes to the *usp39* mutant phenotype

Since *usp39* is known to be an essential component of the RNA splicing machinery, the more than 70% decrease of *rb1* expression in *usp39* mutants may be attributed to defects in RNA splicing. We therefore examined *rb1* splicing status by PCR amplification using primers corresponding to each end of 19 out of 27 exons of the *rb1* gene. Primers designed for exon 3 and exon 4 resulted in a PCR product of 250 base pairs (bp) in wt and mutant embryos, representing a correctly spliced mRNA fragment. However, mutant embryos exhibited an additional larger PCR product of 343 bp (Figure 6F). Further DNA sequence analysis revealed that the 343 bp PCR product derived from *usp39* mutants contain the

Table 2. Summary of cell cycle genes affected in *usp39* mutant embryos from microarray hybridization and confirmed with quantitative RT-PCR.

GB accession	Unigene ID	Location	Gene Symbol	Microarray Ratio	RT-PCR Ratio
NM_213406	Dr.75152	chr11	***cdk2***	0.4	0.18
XM_689974	Dr.13764	chr14	***pttg***	ND	1.3
NM_212564	Dr.24379	chr17	***cdc2***	0.53	0.36
NM_199430	Dr.80580	chr7	***ccnb2***	0.58	0.5
AF398516	Dr.75267	chr25	***cdkn1b***	0.57	0.53
AL912410	Dr.151578	chr22	***cdkn1a***	ND	18
NM_152949	Dr.121874	chr14	***ccna2***	0.5	0.45
NM_131025	Dr.75056	chr7	***ccnd1***	0.82	0.65
NM_130995	Dr.29	chr7	***ccne***	0.52	0.54
NM_213432	Dr.77272	chr25	***e2f4***	2.8	3.09
NM_001077780	Dr.42121	chr21	***rb1***	0.49	0.34
XM_001922133	Dr.79466	chr25	***rbl2***	2.39	ND

ND indicates not determined.

doi:10.1371/journal.pgen.1001271.t002

sequence of an unspliced intron between exon 3 and 4. The splicing defect would lead to a premature stop codon in the intron between exon 3 and exon 4 of *rb1* (data not show), which would lead to nonsense-mediated mRNA decay. We then performed an *rb1* mRNA overexpression experiment in *usp39* mutants and observed partial rescue of the adenohypophysis phenotype (Figure 6I, mutant N = 34, ~50% showed rescue), validating the importance of *usp39*-mediated *rb1* mRNA splicing in controlling pituitary lineage expansion during development. In addition, we performed quantitative RT-PCR analysis on the *rb1* mRNA-injected *usp39* embryos and observed a 30% reduction of *e2f4* expression compared to control uninjected *usp39* mutants (Figure S5A), indicating that *e2f4* upregulation in *usp39* mutant is secondary to Rb1 loss of function. Futhermore, this was confirmed by quantitative RT-PCR analysis on the *e2f4* MO-injected *usp39* embryos and observed that there was no change in *rb1* expression compared to control uninjected *usp39* mutants (Figure S5B).

Discussion

In this study, we identified and functionally characterized the zebrafish *usp39* gene, important for human and yeast pre-mRNA splicing [18,19]. We demonstrated that loss of *usp39* results in defects in *rb1* mRNA splicing and downregulation of *rb1*

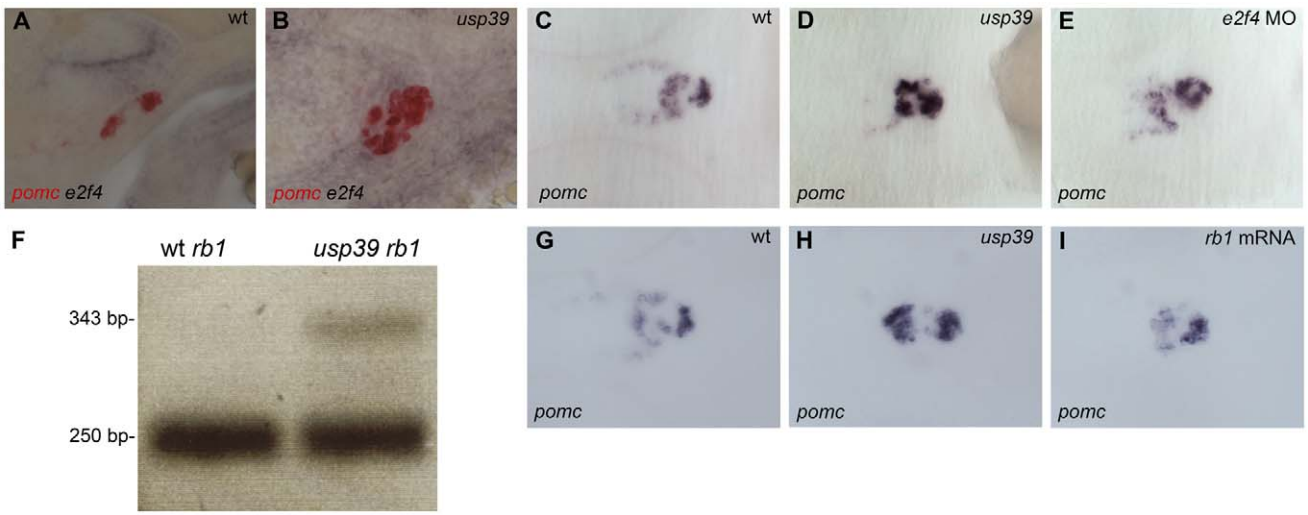

Figure 6. Loss of *usp39* leads to aberrant Rb1 mRNA splicing and increased pituitary *e2f4* expression. A,B: Whole-mount double *in situ* hybridization of *pomc* in red and *e2f4* in purple at 48 hpf, lateral view. (A) Wild-type (wt) embryo. (B) Expression of *e2f4* is higher and colocalizes with *pomc* expression in *usp39* mutant embryos. C–E and G–I: Whole-mount *in situ* hybridization of *pomc* at 48 hpf, ventral view, anterior to left. (C) wt. (D) *usp39* mutant. (E) *e2f4*-MO-injected *usp39* mutant embryos showed partial *pomc* rescue similar to observed in wt embryonic *pomc* expression (C). F: PCR product with primers designed for region between exon 3 and exon 4 of *rb1* in wt and *usp39* mutant embryos. wt embryos only contain a 250 base pair (bp) PCR band, indicating that the intron was correctly spliced out. However, in the *usp39* mutants there is an additional 343 bp band that contains the intron sequence. G–I: (G) wt. (H) *usp39* mutant. (I) *rb1* mRNA-injected *usp39* mutants exhibit partial rescue of *pomc* expression similar to wt embryos (G).

doi:10.1371/journal.pgen.1001271.g006

expression (Figure 6F, Table 2; Figure S3). Both loss of *usp39* as well as *rb1* downregulation in *usp39* mutants may be explained by nonsense-mediated mRNA decay due to a premature termination codon. *RB1* gene mutation leading to pre-mRNA splicing defects have been shown in human cancers [33] and our study suggests a novel mechanism resulting in *rb1* splicing defects due to a *usp39* mutation.

Control of pituitary progenitor cell proliferation in concert with terminal differentiation during embryonic pituitary development is poorly understood. In mouse pituitary primordia, attenuated proliferation of cells destined to become hormone-expressing cell types occurs days before lineage-specific hormones start to express [34]. In contrast, zebrafish pituitary terminal differentiation is initiated while progenitor cells are still organized in a placodal fashion in the anterior neural ridge [2,16]. The *usp39* mutants demonstrated no early difference of adenohypophyseal primordia compared with wt, until 48 hpf when terminally differentiated cells had already migrated to a mature pituitary destination. Pituitary lineage expansion became apparent at 48 hpf in *usp39* mutants, as indicated by expression of pituitary transcription factors and lineage-specific hormone markers (Figure 3 and Figure 5). Similarly, it was found that inactivation of Rb in the small intestines of mice results in increased proliferation of differentiated cells in the villus but not in the stem cells located in the base of the crypts [35]. Therefore, our results suggest that loss of *usp39* does not affect pituitary specification, initiation and early differentiation, but does induce lineage expansion at later development stages when the cells are terminally differentiated.

Our results indicate that *e2f4* overexpression has at least a partial but direct affect on adenohypophyseal cell lineages in *usp39* mutants, as *e2f4* antisense MO knockdown partially reverted the pituitary phenotype of *usp39* mutants (Figure 6 and Figure S4). The *usp39* mutants demonstrated persistently upregulated *e2f4* expression, although molecular mechanisms leading to *e2f4* overexpression remain to be determined. Overexpression of *e2f4* may exert oncogenic activity promoting cell-cycle progression as previously indicated in pituitary, thyroid, lung neuroendocrine hyperplasia [36], intestinal crypt cells, colorectal cancer cells [37] as well as in prostate cancer [38]. We demonstrated an increase of POMC-GFP-positive cells in the *usp39* mutant embryos compare to wt (Figure S2). Consequently, *e2f4* upregulation in *usp39* mutants may contribute to increased proliferation of terminally differentiated pituitary cells leading to lineage expansion as seen in our BrdU studies (Figure S2). On the other hand, E2F4 is a key regulator associated with p130 to promote quiescent G0 and terminal differentiation [13]. The cyclin kinase inhibitor, p21, inhibits decay of the E2F4-p130 complex, promotes senescence and restrains growth, contributing to the benign propensity of pituitary adenomas [39,40]. Our microarray and quantitative RT-PCR data showed increased *cdkn1a (p21)*, *e2f4* and *rbl2* (p130), which may indicate an enhanced quiescent G0 phase inducing terminal differentiation and lineage expansion in *usp39* mutants.

Although the focus of this study was the role of *usp39* in pituitary development, this gene is also expressed in neuronal tissues and when mutated, embryos show microcephaly and smaller eyes, therefore *usp39* function may not be restricted to pituitary development. We propose that *usp39*, through targeting a set of key regulatory genes by modulating RNA splicing, should have a broader role in regulating neuronal cell lineage development. Although how *usp39* controls target mRNA splicing remains to be fully elucidated, the *usp39* ortholog of the yeast protein Sad1p was found to have two roles: it is involved in the assembly of U4 snRNP to U6 snRNP and is also required for splicing [18]. Furthermore, previous reports have shown that a zebrafish RNA splicing factor, *p110*, is required for U4 and U6 snRNPs recycling, and a mutation in *p110* leads to thymic hypoplasia as well as eye and exocrine pancreas defects [41]. In addition, microarray analysis of *p110* mutant shows a compensatory mechanism inducing increased expression of other splicing factors, which may reverse the recycling defects [41]. We observed a similar result in our microarray analysis with upregulation of other U4/U6.U5 tri-snRNP proteins, which suggests a compensatory mechanism in *usp39* mutants (Table S2 and Figure 6F). The human tri-snRNP specific proteins include 65K, 110K and 27K are encoded by USP39, SART1 and SNRNP27, respectively and play a similar role in splicing [21]. Specifically, both *sart1* and *snrnp27* were found to be upregulated in our microarray analysis demonstrating a compensatory role due to the absence of *usp39* (Table S2). Additionally, we discovered another neuronal gene, *otx2*, which was also significantly downregulated due to a splicing defect (Figure S6). However, *otx2* mRNA overexpression in *usp39* mutant embryos did not rescue the pituitary phenotype (data not shown), validating that the Rb1/E2F4 pathway is more specific to pituitary regulation. A systematic analysis of splicing variation of all mRNA transcripts affected by *usp39* deficiency will uncover additional pathways that control neuronal and organ development by RNA splicing mechanisms.

In summary, our findings indicate that *usp39* plays an important role in pituitary development by regulating *rb1* and *e2f4*. Loss of *usp39* leads to pituitary cell lineage expansion through *rb1* downregulation due to a splicing defect. In addition, *e2f4* overexpression contributes to increased pituitary cell mass, likely as a result of increased terminal differentiation or proliferation. Our studies reveal a novel role of *usp39*-mediated mRNA splicing of *rb1* in pituitary cell growth control, which is critical for maintaining embryonic pituitary homeostasis.

Materials and Methods

Mutagenesis and fish husbandry

Mutagenesis with ENU was performed as described [25]. Mutants including *hp689* were identified from random sibling crossing from F2 families giving rise to 25% altered *pomc* expression at 48 hpf.

Genetic mapping

Linkage analysis was established by mating *hp689* heterozygote in an AB background to the WIK strain. Random sibling crossing identified F1 carriers, and mutants were identified phenotypically in F2 offspring at 48 hpf. We analyzed linkage between *hp689* and simple sequence-length polymorphism markers [42]. Linkage analysis found the z34450 marker located 2.4 cM (4 recombinations in 168 meiosis), G40879 marker located 0.3 cM (1 recombination in 288 meioses), ephb4a located 2.2 cM (5 recombinations in 114 meioses) and marker ndrg3 located 0.3cM (1 recombination in 310 meioses) in linkage group 5 (LG5) linked to the mutation.

Genotyping of *usp39* mutants

Total RNA derived from 48 hpf mutant and wild-type embryos was prepared by TRIZOL (Invitrogen) reagent extraction and used to generate cDNA by SuperscriptII reverse transcriptase (Invitrogen) with oligoDT primers (Roche Applied Science). The region near marker *ndrg3* contain 7 genes and sequencing the *usp39* full-length cDNA with primers CGCGTTCACAGTGCGTTC and TTTCTCATTGTGTGTTTTACTCAGTC from mutant embryos revealed a point mutation that converted

a TAT codon into a TAA in Exon 11, resulting in a premature termination codon rather than a tyrosine residue.

Cloning of the zebrafish *usp39* cDNA

The *usp39* full-length cDNA fragment was generated from wild-type embryos as described above and subcloned into pCRII-TOPO.

Morpholino, mRNA synthesis, and microinjection

Antisense MO'swere injected into embryos as described [27]. The sequence of *usp39* MO is 5′-TTCACGCCTCTGATCA-TATTTTAAG-3′ and for *e2f4* MO is 5′-ACTCTCCCAT-CGCTCCCAGGTCGTT-3′ (Gene Tools, Inc). One- to two-cell stage embryo was injected at 3.9 ng for the *usp39* MO and 1.4 ng of *e2f4* MO. The *usp39* overexpression construct was generated by subcloning full-length *usp39* cDNA from vector pCRII-*usp39* into the EcoRI site of vector pXT7. The pXT7-*usp39* vector was linearized with XbaI and mRNA was transcribed using T7 mMessage mMachine kit (Ambion). The *rb1* overexpression construct was generated by subcloning full-length *rb1* cDNA (Accession Number: BC125966, Openbiosystems) to vector $pCS2^{+}$ in the StuI and XhoI sites. The *rb1*-$pCS2^{+}$ vector was then linearized with XbaI and the mRNA transcribed using Sp6 mMessage mMachine kit (Ambion). mRNA injections were performed at the one-cell stage at approximately 200 pg for *usp39* and 267 pg for *rb1*.

RNA *in situ* hybridization

Single and double whole-mount *in situ* hybridizations were performed as described [43]. *usp39* antisense probe was synthesized from pCRII-*usp39* with Sp6 RNA polymerase after linearization with NotI. The following riboprobes were generated from cDNAs as described: *pomc* [16], *gh*, *prl*, *tshβ*, *lim3*, *pit1* and *pitx3* [2], *eya1* [44], *crh* [29], *gnrh2* and *gnrh3* [30], and *ascl1a* [31]. Full-length cDNA for *cga* (Accession Number: BC116611) and *e2f4* (Accession Number: BC056832) were purchased from Open-biosystems. *e2f4* was subcloned to pCRII-TOPO vector and linearized with SpeI whereas the *cga*-Express1 was linearized with EcoRI and riboprobes were synthesized with T7 RNA polymerase.

Antibody staining

Whole-mount antibody staining was performed using a rabbit anti-tyrosine hydroxylase (TH) primary antibody at 1:200 dilution (Chemicon) and detected with an Alexa (A594)-conjugated goat anti-rabbit secondary antibody at 1:200 dilution (Molecular Probes).

Microarray analysis

Total RNA from 48 hpf *usp39* mutants and wild-type embryos was prepared and microarray performed as described [45].

Quantitative RT-PCR

cDNA was generated as described above. RT-PCR was performed using the iCycler iQ Real-Time PCR Detection System (BioRad) and the iQ SYBR Green Supermix (Biorad). Relative cDNA amounts were calculated using the iCycler program (BioRad) and gene expression levels measured by the $2^{-\Delta\Delta CT}$ method [46], comparing *usp39* mutant embryos to WT controls, with *β-actin* used as the reference gene. This procedure was repeated three times for each gene with three different experimental cDNA pools. At least three replicates were used for each cDNA pool. Gene expression was reported as relative expression change in *usp39* mutants over WT embryos ± standard error (for primer sequences see Table S1).

Retinoblastoma splicing primers

cDNA was generated as described above. We designed primers that covered the exon and intron region of Exon 3 to Exon 4 of the *rb1* gene. The primers used were: CCGTATTCGAACAGA-CAGCA and GGTAGAGGGCCAAAGTCACA.

Vibratome sections

After whole-mount *in situ* hybridization, embryos were washed in PBS, manually deyolked, and mounted on their lateral side in 4% low melting agarose (Fisher Scientific) in PBS. Thin 100 µm slices were cut using a vibratome (Vibratome 1000 Plus) and sections were stored in PBS until imaging.

Image acquisition and processing

The *in situ* hybridization and the vibratome sections were imaged with an Axiocam digital camera (Zeiss) mounted on an Axioplan 2 compound microscope (Zeiss). OpenLab 4.0.2 software (Improvision) was used to capture all images; Photoshop CS4 software (Adobe Systems) was used for further image processing.

Supporting Information

Figure S1 *lim3* expression is not altered at 36 hpf. (A, B) Whole-mount *in situ* hybridization with *lim3* probe, ventral view with anterior to left. (A) wild-type (wt). (B) Expression of *lim3* in *usp39* mutant embryos is not changed compared to wt embryos at 36 hpf.
Found at: doi:10.1371/journal.pgen.1001271.s001 (1.30 MB TIF)

Figure S2 Increase in pituitary cell number in *usp39* mutants compared to wt embryos. Immunocytochemistry using anti-GFP antibody was performed on 5 µm frontal sections of wt and *usp39* mutants with a POMC-GFP transgenic background at 48 hpf, ventral view, anterior on top. The anti-GFP, rabbit IgG fraction, Alexa Fluor 488 conjugated antibody are at 1:200 dilution (Invitrogen). A drop of ProLong Gold antifade reagent with DAPI (Invitrogen) was added to sections and coverslipped. (A, B) All pituitary POMC-GFP-positive cells are included in two sequential sections of the wild-type embryos. (C–E) Three sections are required to include all pituitary POMC-GFP positive cells in *usp39* mutant embryos. (F) Four wt and four *usp39* mutants were analyzed for POMC-GFP-positive cells. *usp39* mutants had an average of 25.5 POMC-GFP-positive cells compare to 12.5 in wt embryos (mean ± SEM; $p<0.02$, $n=4$). (G) To determine the total number of pituitary cells, DAPI positive cells were counted in the same sections of the four wt and four *usp39* mutants. *usp39* mutants had an average of 123.5 DAPI-positive cells in the pituitary compare to 48.25 in wt embryos (mean ± SEM; $p<0.03$, $n=4$). (H–I) Embryos were placed in 10 mM solution of BrdU (Sigma) in fish water at 10-somite stage and kept in dark until 48 hpf. The embryos were also injected with 10 nl of 10 mM Brdu at 24 hfp. BrdU labeling results in 48 hpf embryos by immunocytochemistry using anti-GFP antibody and anti-BrdU was performed in whole-mount embryos as described in [Liu et al]. The anti-GFP, rabbit IgG fraction and Alexa Fluor 488 secondary antibody are at 1:200 dilution (Invitrogen). The anti-BrdU, mouse IgG fraction (Santa Cruz) and Alexa Fluor 594 secondary antibody (Invitrogen) are at 1:100 and 1:200 dilution, respectively. Imaging was performed on vibratome 100 µm sections of wt and *usp39* mutant embryos. (H) Proliferating cells in the pituitary were not evident in wt embryos. (I) *usp39* mutant embryos contain a

higher number of proliferating cells in the pituitary region marked by white arrowheads. [Liu NA, Ren M, Song J, Rios Y, Wawrowsky K, et al. (2008) In vivo time-lapse imaging delineates the zebrafish pituitary proopiomelanocortin lineage boundary regulated by FGF3 signal. Dev Biol.]
Found at: doi:10.1371/journal.pgen.1001271.s002 (9.15 MB TIF)

Figure S3 Quantitative RT-PCR analysis showing expression of cell cycle regulators with loss of *usp39*. Relative gene expression levels were calculated for *usp39* mutant embryos compared to control WT embryos (see Materials and Methods). Dashed line represents a value of 1, which corresponds to no change in WT expression. Significant change was determined by two standard deviations (Mean ± SEM).
Found at: doi:10.1371/journal.pgen.1001271.s003 (9.64 MB TIF)

Figure S4 *e2f4* morpholino injections rescued *prl* expression in *usp39* mutants. (A–C) Whole-mount *in situ* hybridization with *prl* probe, ventral view with anterior to left. (A) wt. (B) *usp39* mutant embryo. (C) Expression of *prl* in *e2f4*-MO-injected *usp39* embryos was partially rescued.
Found at: doi:10.1371/journal.pgen.1001271.s004 (9.55 MB TIF)

Figure S5 *e2f4* mRNA expression is partially rescued by *rb1* mRNA overexpression in *usp39* mutant embryos while *e2f4* MO injections did not rescue *rb1* mRNA levels. A 30% decrease of *e2f4* expression was detected in the *rb1* mRNA injected *usp39* embryos compared to control uninjected *usp39* mutants by quantitative RT-PCR (mean ± SEM; n = 60 embryos; $p<0.03$). (B) However, the expression of *rb1* mRNA levels by quantitative RT-PCR of *usp39* mutants injected with *e2f4* morpholino did not change (mean ± SEM; n = 67 embryos).
Found at: doi:10.1371/journal.pgen.1001271.s005 (9.49 MB TIF)

Figure S6 *otx2* splicing defect in *usp39* mutants. (A, B) Whole-mount *in situ* hybridization of *otx2* at 48 hpf, ventral view, anterior to left. (A) wt. (B) Expression of *otx2* is downregulated in *usp39* mutants. (C) PCR product with primers designed for a region between exon 3 and exon 4 of *otx2* in wt and *usp39* mutant embryos. In addition to the 79 bp band in wt, the *usp39* mutant embryos contain an additional 289 bp band, which corresponds to a mispliced mRNA fragment including the intron between exon 3 and 4. The primers used were: GGCCTTGAAAATCAACTTGC and CTGCTGTTGGCGACACTTT.
Found at: doi:10.1371/journal.pgen.1001271.s006 (9.49 MB TIF)

Table S1 Quantitative RT-PCR primers.
Found at: doi:10.1371/journal.pgen.1001271.s007 (0.05 MB DOC)

Table S2 Tri-snRNP factors affected in *usp39* mutants.
Found at: doi:10.1371/journal.pgen.1001271.s008 (0.04 MB DOC)

Acknowledgments

We thank Shawn Burgess for conducting the microarray analysis, Anqi Liu and Yuan Dong for assistance with animal husbandry, and Hong Jiang for technical support.

Author Contributions

Conceived and designed the experiments: YR NAL SL. Performed the experiments: YR. Analyzed the data: YR SM NAL SL. Wrote the paper: YR NAL SL.

References

1. Wells S, Murphy D (2003) Transgenic studies on the regulation of the anterior pituitary gland function by the hypothalamus. Front Neuroendocrinol 24: 11–26.
2. Pogoda HM, Hammerschmidt M (2007) Molecular genetics of pituitary development in zebrafish. Semin Cell Dev Biol 18: 543–558.
3. Melmed S (2003) Mechanisms for pituitary tumorigenesis: the plastic pituitary. J Clin Invest 112: 1603–1618.
4. Krude H, Biebermann H, Gruters A (2003) Mutations in the human proopiomelanocortin gene. Ann N Y Acad Sci 994: 233–239.
5. Drouin J, Bilodeau S, Vallette S (2007) Of old and new diseases: genetics of pituitary ACTH excess (Cushing) and deficiency. Clin Genet 72: 175–182.
6. Melmed S (2009) Acromegaly pathogenesis and treatment. J Clin Invest 119: 3189–3202.
7. Chen HZ, Tsai SY, Leone G (2009) Emerging roles of E2Fs in cancer: an exit from cell cycle control. Nat Rev Cancer 9: 785–797.
8. Jacks T, Fazeli A, Schmitt EM, Bronson RT, Goodell MA, et al. (1992) Effects of an Rb mutation in the mouse. Nature 359: 295–300.
9. Lee EY, Cam H, Ziebold U, Rayman JB, Lees JA, et al. (2002) E2F4 loss suppresses tumorigenesis in Rb mutant mice. Cancer Cell 2: 463–472.
10. Moberg K, Starz MA, Lees JA (1996) E2F-4 switches from p130 to p107 and pRB in response to cell cycle reentry. Mol Cell Biol 16: 1436–1449.
11. Rayman JB, Takahashi Y, Indjeian VB, Dannenberg JH, Catchpole S, et al. (2002) E2F mediates cell cycle-dependent transcriptional repression in vivo by recruitment of an HDAC1/mSin3B corepressor complex. Genes Dev 16: 933–947.
12. Humbert PO, Rogers C, Ganiatsas S, Landsberg RL, Trimarchi JM, et al. (2000) E2F4 is essential for normal erythrocyte maturation and neonatal viability. Mol Cell 6: 281–291.
13. Vairo G, Livingston DM, Ginsberg D (1995) Functional interaction between E2F-4 and p130: evidence for distinct mechanisms underlying growth suppression by different retinoblastoma protein family members. Genes Dev 9: 869–881.
14. Ginsberg D, Vairo G, Chittenden T, Xiao ZX, Xu G, et al. (1994) E2F-4, a new member of the E2F transcription factor family, interacts with p107. Genes Dev 8: 2665–2679.
15. Beijersbergen RL, Kerkhoven RM, Zhu L, Carlee L, Voorhoeve PM, et al. (1994) E2F-4, a new member of the E2F gene family, has oncogenic activity and associates with p107 in vivo. Genes Dev 8: 2680–2690.
16. Liu NA, Huang H, Yang Z, Herzog W, Hammerschmidt M, et al. (2003) Pituitary corticotroph ontogeny and regulation in transgenic zebrafish. Mol Endocrinol 17: 959–966.
17. Liu NA, Liu Q, Wawrowsky K, Yang Z, Lin S, et al. (2006) Prolactin receptor signaling mediates the osmotic response of embryonic zebrafish lactotrophs. Mol Endocrinol 20: 871–880.
18. Lygerou Z, Christophides G, Seraphin B (1999) A novel genetic screen for snRNP assembly factors in yeast identifies a conserved protein, Sad1p, also required for pre-mRNA splicing. Mol Cell Biol 19: 2008–2020.
19. Makarova OV, Makarov EM, Luhrmann R (2001) The 65 and 110 kDa SR-related proteins of the U4/U6.U5 tri-snRNP are essential for the assembly of mature spliceosomes. EMBO J 20: 2553–2563.
20. Valadkhan S (2007) The spliceosome: caught in a web of shifting interactions. Curr Opin Struct Biol 17: 310–315.
21. Liu S, Rauhut R, Vornlocher HP, Luhrmann R (2006) The network of protein-protein interactions within the human U4/U6.U5 tri-snRNP. RNA 12: 1418–1430.
22. van Leuken RJ, Luna-Vargas MP, Sixma TK, Wolthuis RM, Medema RH (2008) Usp39 is essential for mitotic spindle checkpoint integrity and controls mRNA-levels of aurora B. Cell Cycle 7: 2710–2719.
23. Driever W, Solnica-Krezel L, Schier AF, Neuhauss SC, Malicki J, et al. (1996) A genetic screen for mutations affecting embryogenesis in zebrafish. Development 123: 37–46.
24. Haffter P, Granato M, Brand M, Mullins MC, Hammerschmidt M, et al. (1996) The identification of genes with unique and essential functions in the development of the zebrafish, Danio rerio. Development 123: 1–36.
25. Kim HJ, Sumanas S, Palencia-Desai S, Dong Y, Chen JN, et al. (2006) Genetic analysis of early endocrine pancreas formation in zebrafish. Mol Endocrinol 20: 194–203.
26. Bairoch A, Bucher P, Hofmann K (1996) The PROSITE database, its status in 1995. Nucleic Acids Res 24: 189–196.
27. Nasevicius A, Ekker SC (2000) Effective targeted gene 'knockdown' in zebrafish. Nat Genet 26: 216–220.
28. Ben-Jonathan N, Hnasko R (2001) Dopamine as a prolactin (PRL) inhibitor. Endocr Rev 22: 724–763.
29. Chandrasekar G, Lauter G, Hauptmann G (2007) Distribution of corticotropin-releasing hormone in the developing zebrafish brain. J Comp Neurol 505: 337–351.

30. Steven C, Lehnen N, Kight K, Ijiri S, Klenke U, et al. (2003) Molecular characterization of the GnRH system in zebrafish (Danio rerio): cloning of chicken GnRH-II, adult brain expression patterns and pituitary content of salmon GnRH and chicken GnRH-II. Gen Comp Endocrinol 133: 27–37.
31. Allende ML, Weinberg ES (1994) The expression pattern of two zebrafish achaete-scute homolog (ash) genes is altered in the embryonic brain of the cyclops mutant. Dev Biol 166: 509–530.
32. Quereda V, Malumbres M (2009) Cell cycle control of pituitary development and disease. J Mol Endocrinol 42: 75–86.
33. Zhang K, Nowak I, Rushlow D, Gallie BL, Lohmann DR (2008) Patterns of missplicing caused by RB1 gene mutations in patients with retinoblastoma and association with phenotypic expression. Hum Mutat 29: 475–484.
34. Seuntjens E, Denef C (1999) Progenitor cells in the embryonic anterior pituitary abruptly and concurrently depress mitotic rate before progressing to terminal differentiation. Mol Cell Endocrinol 150: 57–63.
35. Chong JL, Wenzel PL, Saenz-Robles MT, Nair V, Ferrey A, et al. (2009) E2f1-3 switch from activators in progenitor cells to repressors in differentiating cells. Nature 462: 930–934.
36. Parisi T, Bronson RT, Lees JA (2009) Inhibition of pituitary tumors in Rb mutant chimeras through E2f4 loss reveals a key suppressive role for the pRB/E2F pathway in urothelium and ganglionic carcinogenesis. Oncogene 28: 500–508.
37. Garneau H, Paquin MC, Carrier JC, Rivard N (2009) E2F4 expression is required for cell cycle progression of normal intestinal crypt cells and colorectal cancer cells. J Cell Physiol 221: 350–358.
38. Waghray A, Schober M, Feroze F, Yao F, Virgin J, et al. (2001) Identification of differentially expressed genes by serial analysis of gene expression in human prostate cancer. Cancer Res 61: 4283–4286.
39. Smith EJ, Leone G, DeGregori J, Jakoi L, Nevins JR (1996) The accumulation of an E2F-p130 transcriptional repressor distinguishes a G0 cell state from a G1 cell state. Mol Cell Biol 16: 6965–6976.
40. Chesnokova V, Zonis S, Kovacs K, Ben-Shlomo A, Wawrowsky K, et al. (2008) p21(Cip1) restrains pituitary tumor growth. Proc Natl Acad Sci U S A 105: 17498–17503.
41. Trede NS, Medenbach J, Damianov A, Hung LH, Weber GJ, et al. (2007) Network of coregulated spliceosome components revealed by zebrafish mutant in recycling factor p110. Proc Natl Acad Sci U S A 104: 6608–6613.
42. Shimoda N, Knapik EW, Ziniti J, Sim C, Yamada E, et al. (1999) Zebrafish genetic map with 2000 microsatellite markers. Genomics 58: 219–232.
43. Hauptmann G, Gerster T (2000) Multicolor whole-mount in situ hybridization. Methods Mol Biol 137: 139–148.
44. Sahly I, Andermann P, Petit C (1999) The zebrafish eya1 gene and its expression pattern during embryogenesis. Dev Genes Evol 209: 399–410.
45. Gomez GA, Veldman MB, Zhao Y, Burgess S, Lin S (2009) Discovery and characterization of novel vascular and hematopoietic genes downstream of etsrp in zebrafish. PLoS ONE 4: e4994. doi:10.1371/journal.pone.0004994.
46. Schmittgen TD, Livak KJ (2008) Analyzing real-time PCR data by the comparative C(T) method. Nat Protoc 3: 1101–1108.